Cell Death and Differentiation (2015) 22, 1577–1589

www.nature.com/cdd

E2F1 and E2F2 prevent replicative stress and subsequent p53-dependent organ involution

A Iglesias-Ara[1,3], O Zenarruzabeitia[1,3,4], L Buelta[2], J Merino[2] and AM Zubiaga*[,1]

Tissue homeostasis requires tight regulation of cellular proliferation, differentiation and apoptosis. E2F1 and E2F2 transcription factors share a critical role in tissue homeostasis, since their combined inactivation results in overall organ involution, specially affecting the pancreatic gland, which subsequently triggers diabetes. We have examined the mechanism by which these E2Fs regulate tissue homeostasis. We show that pancreas atrophy in E2F1/E2F2 double-knockout (DKO) mice is associated with mitochondrial apoptosis and activation of the p53 pathway in young animals, before the development of diabetes. A deregulated expression of E2F target genes was detected in pancreatic cells of young DKO animals, along with unscheduled DNA replication and activation of a DNA damage response. Importantly, suppression of DNA replication *in vivo* with aphidicolin led to a significant inhibition of the p53 pathway in DKO pancreas, implying a causal link between DNA replication stress and p53 activation in this model. We further show that activation of the p53 pathway has a key role in the aberrant phenotype of DKO mice, since targeted inactivation of p53 gene abrogated cellular apoptosis and prevented organ involution and insulin-dependent diabetes in mice lacking E2F1/E2F2. Unexpectedly, p53 inactivation unmasked oncogenic features of E2F1/E2F2-depleted cells, as evidenced by an accelerated tumor development in triple-knockout mice compared with $p53^{-/-}$ mice. Collectively, our data reveal a role for E2F1 and E2F2 as suppressors of replicative stress in differentiating cells, and uncover the existence of a robust E2F-p53 regulatory axis to enable tissue homeostasis and prevent tumorigenesis. These findings have implications in the design of approaches targeting E2F for cancer therapy.
Cell Death and Differentiation (2015) **22,** 1577–1589; doi:10.1038/cdd.2015.4; published online 6 February 2015

The challenges that cells face to maintain a differentiated status within a tissue entail overcoming a number of obstacles, such as uncontrolled proliferation, damaged organelles, ROS or DNA breaks. Aberrant cells can activate surveillance pathways to be eliminated, or they may, alternatively, accumulate. Lack of balance between these two decisions results in tissue degeneration or in tumorigenesis. Cancer cells commonly exhibit deregulation of a functional pRb pathway.[1] Such deregulation can occur at multiple points of the pathway, including mutations or deletions of pRb gene itself, activation of cyclin/CDKs that phosphorylate and thereby functionally inactivate pRb, or inactivation of CDK inhibitors, such as $p16^{INK4A}$.[2] The oncogenic stress induced by loss of pRb function is known to activate the other major tumor suppressor, p53.[2] Activated p53 can, depending on the cellular context, induce cell-cycle arrest, senescence or apoptosis as a failsafe mechanism against tumorigenesis, and the combined loss of pRb and p53 pathways leave cells prone to tumorigenesis. Conversely, hiperactivation of the p53 pathway upon oncogenic stress induced by pRb loss prevents tumor development, yet premature aging may arise leading to a reduction in lifespan.[3]

An extensively characterized function of pRb involves its interaction with members of the E2F family of transcription factors, whereby hypophosphorylated pRb protein forms a complex with E2F members and blocks their transcriptional activity, preventing entry into the cell cycle.[4] Cyclin/CDK-mediated phosphorylation of pRb during G1 releases E2F, thus allowing gene transcription and cell-cycle progression. Inactivation of the pRb pathway is thought to lead to inappropriate activation of E2F factors, followed by increased cellular proliferation rates and tumorigenesis.[5] Thus, inhibition of E2F activity has been proposed as a therapeutic strategy for the treatment of cancer.[6] Mammalian E2F comprises a family of eight transcription factors, originally discovered for their crucial role in the control of cell-cycle progression through the regulation of a large set of responsive genes.[7–9] Subsequently, it was shown that E2Fs also have essential roles in a wide range of functions such as differentiation, apoptosis and DNA repair, underlying their relevance in tissue homeostasis.[8–10]

E2F1 and E2F2 are known to function both as transcriptional activators and as repressors of their target genes, including those coding for microRNAs.[11–15] Moreover, E2F1

[1]Department of Genetics, Physical Anthropology and Animal Physiology, University of the Basque Country, UPV/EHU, Bilbao, Spain and [2]University of Cantabria-IDIVAL, Cantabria, Spain
*Corresponding author: AM Zubiaga, Department of Genetics, Physical Anthropology and Animal Physiology, University of the Basque Country, UPV/EHU, Bilbao 48080, Spain. Tel: +34 94 601 2603; Fax: +34 94 601 3143; E-mail: ana.zubiaga@ehu.es
[3]AI-A and OZ share first authorship.
[4]Current address: BioCruces Health Research Institute, Barakaldo, Spain; and Basque Center for Transfusion and Human Tissues, Galdakao, Spain.
Abbreviations: DKO, double knockout; pRb, retinoblastoma protein; NAO, nonyl-acrydine-orange; ROS, reactive oxygen species; pH3, phospho-histone H3; DDR, DNA damage response; BrdU, bromodeoxyuridine; TKO, triple knockout; MDP, Mandibular hypoplasia, Deafness and Progeroid features; TDT, Terminal Deoxynucleotidyl Transferase; i.p., intraperitoneal; KHB, Krebs-Henseleit bicarbonate; CCCP, carbonyl cyanide m-chloro phenyl hydrazone
Received 03.10.14; revised 19.12.14; accepted 06.1.15; Edited by S Fulda; published online 06.2.15

and E2F2 perform positive as well as negative regulatory roles in cellular proliferation, which appear to be cell specific and context dependent. They have been reported to promote cell-cycle entry and progression upon their ectopic expression.[16] By contrast, targeted inactivation of these E2Fs revealed their essential role in sustaining quiescence in hematopoietic cells,[11] in supporting survival of progenitor cells[16] or in facilitating exit from the cell cycle in differentiating cells.[13,17] However, the mechanisms by which E2F1 and E2F2 accomplish such diverse functions remain unresolved.

The pancreas has emerged as an optimal system to unravel the role of E2F1 and E2F2 in the maintenance of tissue homeostasis. We and others have previously reported that combined inactivation of E2F1 and E2F2 transcription factors leads to exocrine and endocrine pancreatic dysfunction, causing diabetes and the collapse of the entire pancreas.[18,19] After a period of strong cell division cycles, which take place during embryonic development and finalize by the second week after birth, pancreatic tissue is virtually post-mitotic.[20] By contrast, pancreatic cells lacking E2F1 and E2F2 continue cycling aberrantly well beyond this age.[19] Strikingly, E2F1/E2F2 mutant pancreas exhibits an increased apoptotic rate and the organ degenerates rapidly.[19] Other organs in E2F1/E2F2 DKO mice also show a singular involution, particularly the hematopoietic system, salivary glands and testicles,[19] although the mediators involved in E2F1/E2F2-dependent tissue atrophy have not yet been identified.

Here, we explore the mechanism by which E2F1 and E2F2 regulate tissue homeostasis. We show that inactivation of E2F1 and E2F2 results in accumulation of DNA replication mediators, activation of the DNA damage response (DDR) and induction of p53-dependent apoptosis. Genetic elimination of p53 abrogates apoptosis and pancreatic gland involution, and rescues insulin-dependent diabetes. Importantly, the absence of p53 also uncovers oncogenic features of E2F1/E2F2-depleted cells. Collectively, our data stress the relevance of E2F1 and E2F2 as suppressors of replicative stress and regulators of cell-cycle exit during differentiation, and reveal the existence of a robust E2F-p53 regulatory axis to ensure proper organ function and prevent tumorigenesis.

Results

Apoptosis in pancreas lacking E2F1 and E2F2 is associated with p53 accumulation. E2F1/E2F2 double-knockout (DKO) pancreatic cells exhibit increased rates of apoptosis as early as postnatal day 15, before manifestations of pancreatic atrophy.[19] To characterize the apoptotic cell death, we isolated pancreatic cells from 2-week-old DKO and wild-type mice and measured changes in mitochondrial membrane potential by examining fluorescence of cells incubated with JC-1 (Figure 1a). In live cells, JC-1 monomers form aggregates and emit both green and red fluorescence, while in dying cells with collapsed $\Delta\psi_m$, JC-1 is only monomeric and emits exclusively green fluorescence. The percentage of cells positive for green fluorescence and negative for red fluorescence was substantially higher in DKO samples compared with wild-type controls ($45.46 \pm 7.06\%$ *versus* $15.51 \pm 1.07\%$), suggesting mitochondrial apoptosis. Consistent with this result, we detected a reduction of mitochondrial mass in DKO pancreatic cells, as evidenced by the marked difference in fluorescence intensity between DKO and wild-type samples treated with the cardiolipin-binding molecule Nonyl-Acrydine-Orange (NAO) (Figure 1b). To get an insight into the underlying mechanism of apoptosis, we examined p53 protein expression. Accumulation of p53 was detected in the pancreas of DKO mice (Figure 1c). Furthermore, typical p53 direct transcriptional target genes involved in intrinsic (*Bax*, *Puma*, *Apaf-1*, *Pidd*) and extrinsic (*Dr5*) pathways were significantly overexpressed in DKO samples (Figure 1d). Taken together, these results suggest that E2F1/E2F2 double-deficient pancreatic cells undergo apoptosis as a result of p53 protein accumulation and activation.

The levels of p53 can be increased in cells by diverse mechanisms, some of which are mediated by E2F target genes, including $p19^{ARF}$, Sirt1 and Sirt3.[21,22] To assess their role in p53 accumulation in our model, we analyzed the expression of these genes in E2F1/E2F2-depleted cells. The expression of $p19^{ARF}$ was reduced in DKO pancreas, at both the mRNA and protein levels (Figures 1e and f). Additionally, Sirt1 and Sirt3 mRNA levels remained unchanged in DKO samples compared with WT controls (Figure 1e), and no p53 hyperacetylation was observed (Figure 1f). These results rule out a role for $p19^{ARF}$ and Sirt proteins in the accumulation of p53 displayed by DKO pancreases.

We also examined levels of reactive oxygen species (ROS), which are known to activate p53 *via* Apex1.[23] However, ROS or Apex1 protein accumulation was not detected in young DKO mice (Figures 1f and g), and only older diabetic DKO mice showed elevated ROS accumulation (Figure 1g), indicating that activation of p53 pathway in DKO pancreas is not ROS dependent.

Deregulated E2F target gene expression and aberrant cell-cycle control in pancreas of mice deficient in E2F1 and E2F2. To further characterize the phenotype observed in E2F1/E2F2-depleted pancreatic cells, we analyzed DNA synthesis in pancreas of 2-week-old mice. By this age, wild-type pancreas is virtually post-mitotic. As expected, DNA synthesis was essentially undetectable in WT controls (Figure 2a). In contrast, unscheduled DNA replication was detected in E2F1/E2F2 DKO cells. Consistent with these results, we detected an upregulated expression of E2F target genes that promote DNA synthesis and positively regulate G1/S transition and mitosis (Figure 2b).

We also examined the expression of E2F targets that encode CDK regulators. The levels of $p16^{INK4A}$ and $p27^{KIP1}$ were unchanged in DKO cells relative to WT samples. By contrast, the expression of $p21^{CIP1}$ and Cdc25a was increased in DKO cells and the expression of the G1 CDKi $p18^{INK4C}$ was significantly reduced (Figure 2b).

Elevated levels of phosphorylated pRb (Ser807/811 and Ser780) were detected in DKO pancreatic cells, suggesting hyperactivation of G1 cyclin/CDK function. Similarly, mitotic cyclin/CDK activity appeared significantly elevated in DKO cells, as evidenced by the near disappearance of the Cdk1 inhibitory Tyr15 phosphorylation, the increased levels of cyclin

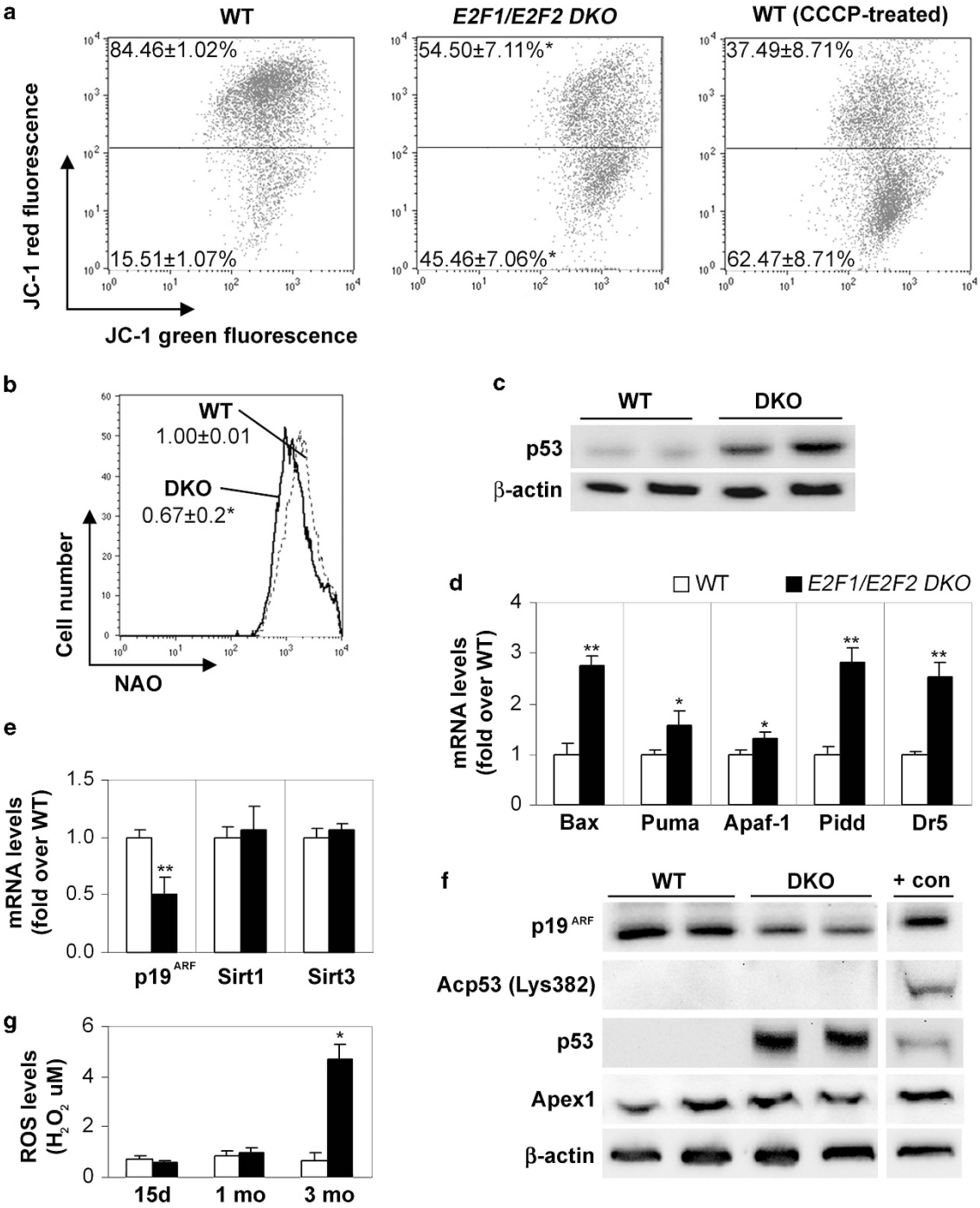

Figure 1 Apoptosis in pancreas deficient in E2F1 and E2F2 is associated with p53 accumulation. (**a**) FACS analysis on freshly isolated WT and DKO pancreatic cells (from 2-week-old mice) stained with JC-1 under basal conditions or after treatment with the mitochondrial uncoupler carbonyl cyanide m-chloro phenyl hydrazone (CCCP) as a control for loss of mitochondrial membrane potential. Cells with compromised mitochondrial membrane potential shift from greenish orange (upper panel) to green (lower panel). Numbers inside each panel represent the percentage of cells (mean ± S.D.) from three independent experiments.*$P<0.002$ *versus* basal WT. (**b**) FACS analysis of mitochondrial mass on freshly isolated WT and DKO pancreatic cells stained with NAO. Results are expressed as fold over NAO fluorescence obtained in WT cells (mean ± S.D.) from three independent experiments. *$P<0.05$. (**c**) Representative western blot analysis of p53 in extracts prepared from 2-week-old WT and DKO pancreas (2 mice/genotype). Expression of β-actin was used as a loading control. (**d**) Reverse transcription Q-PCR analysis of indicated genes in 1-month-old WT and DKO pancreas. *Gapdh* was used as a normalization control. Results are expressed as fold over WT (mean ± S.D.) from three mice per genotype.*$P<0.05$, **$P<0.01$. (**e**) Reverse transcription Q-PCR analysis of of indicated genes in 2-week-old WT and DKO pancreas. *Gapdh* was used as a normalization control. Results are expressed as fold over WT (mean ± S.D.) from three mice per genotype. **$P<0.01$. (**f**) Representative western blot analysis of indicated proteins in extracts prepared from 2-week-old WT and DKO pancreas (2 mice/genotype). Cell extracts from cultured cells that express the analyzed proteins were used as positive controls (+ con) and were run along with the samples. Expression of β-actin was used as a loading control. (**g**) Concentration of ROS in pancreas of WT and DKO mice analyzed at different ages, as described in Materials and Methods. For each age and genotype three mice were analyzed. *$P<0.0001$

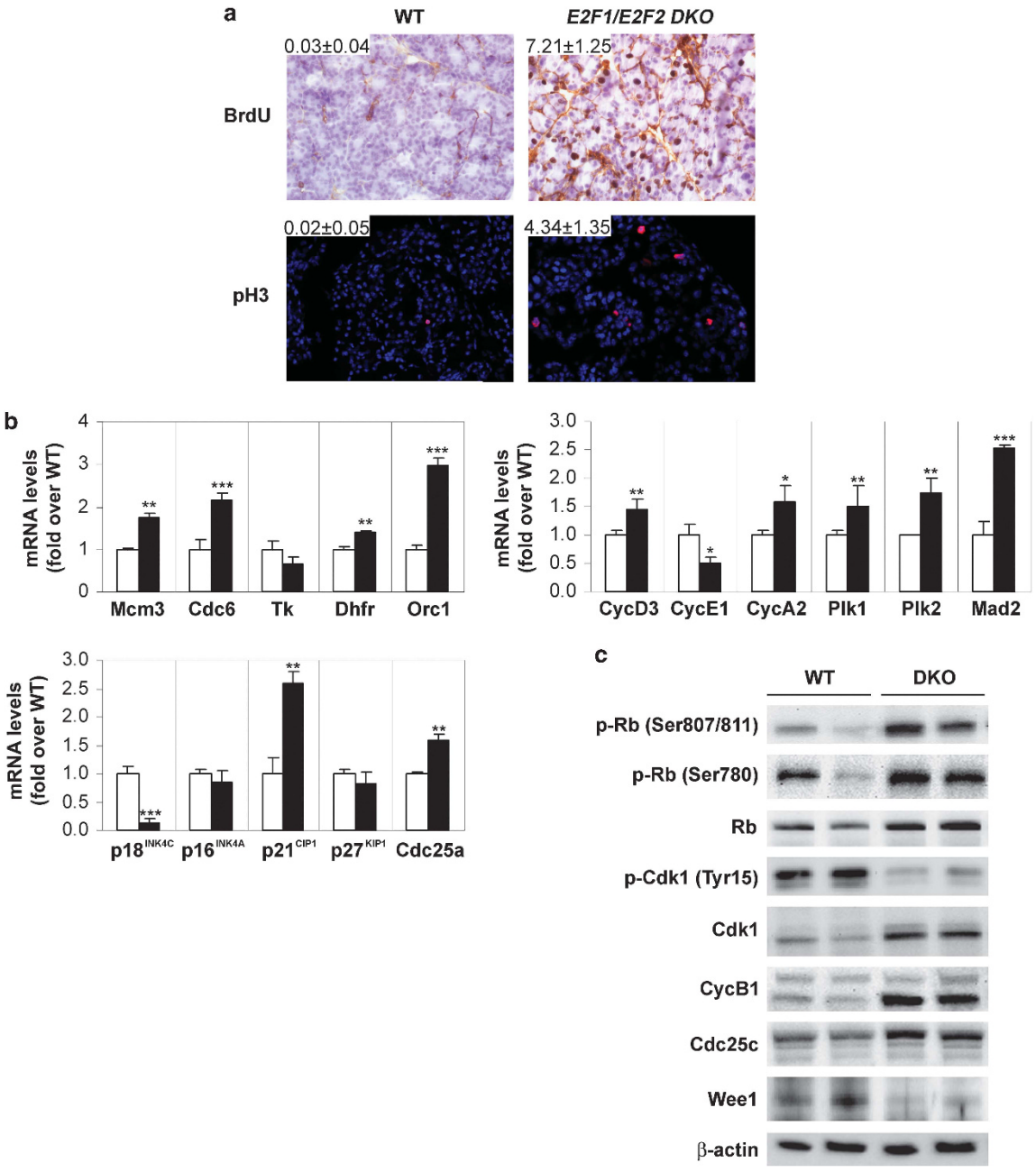

Figure 2 Pancreas of E2F1/E2F2 DKO mice exhibits evidence of inappropriate progression through the cell cycle and replicative stress. (**a**) Immunohistochemical analyses to identify BrdU-positive (upper panels) or pH3-positive (lower panels) nuclei in the pancreas of 2-week-old WT and DKO mice. As shown, DKO mice have an increased number of BrdU-positive as well as pH3-positive cells (x20). The percentages of positive nuclei are indicated (mean ± S.D.). (**b**) Reverse transcription Q-PCR expression analysis of indicated genes in 2-week-old WT and DKO pancreas. *Gapdh* was used as a normalization control. Results are expressed as fold over WT (mean ± S.D.) from three mice per genotype. *$P<0.05$, **$P<0.01$, ***$P<0.0001$. (**c**) Representative western blot analysis of the indicated proteins in extracts prepared from 2-week-old WT and DKO pancreas (2 mice/genotype). Expression of β-actin was used as a loading control

B1 and Cdc25c, and the nearly complete absence of Wee1 protein (Figure 2c). An increased Cdk1 activity is consistent with the accumulation of the mitotic marker phospho-histone H3 (pH3) that was noted in DKO pancreas (Figure 2a). Taken together, these findings suggest that terminally differentiating DKO pancreatic cells are progressing aberrantly through the cell cycle in the absence of repressive signals emanated from E2F1 and E2F2 to promote cell-cycle exit.

p53 accumulation in the pancreas of DKO mice is linked to DNA replication stress. Given the aberrant cyclin/CDK activity observed in DKO samples, we examined DNA damage response (DDR) in pancreas by assessing accumulation of γ-H2AX, a marker for DNA breaks. Western blotting of pancreatic lysates from 7-day-old mice did not show global accumulation of γ-H2AX. However, the levels of γ-H2AX increased significantly in 15-day-old DKO mice and were dramatically higher in adult mice (Figure 3a).

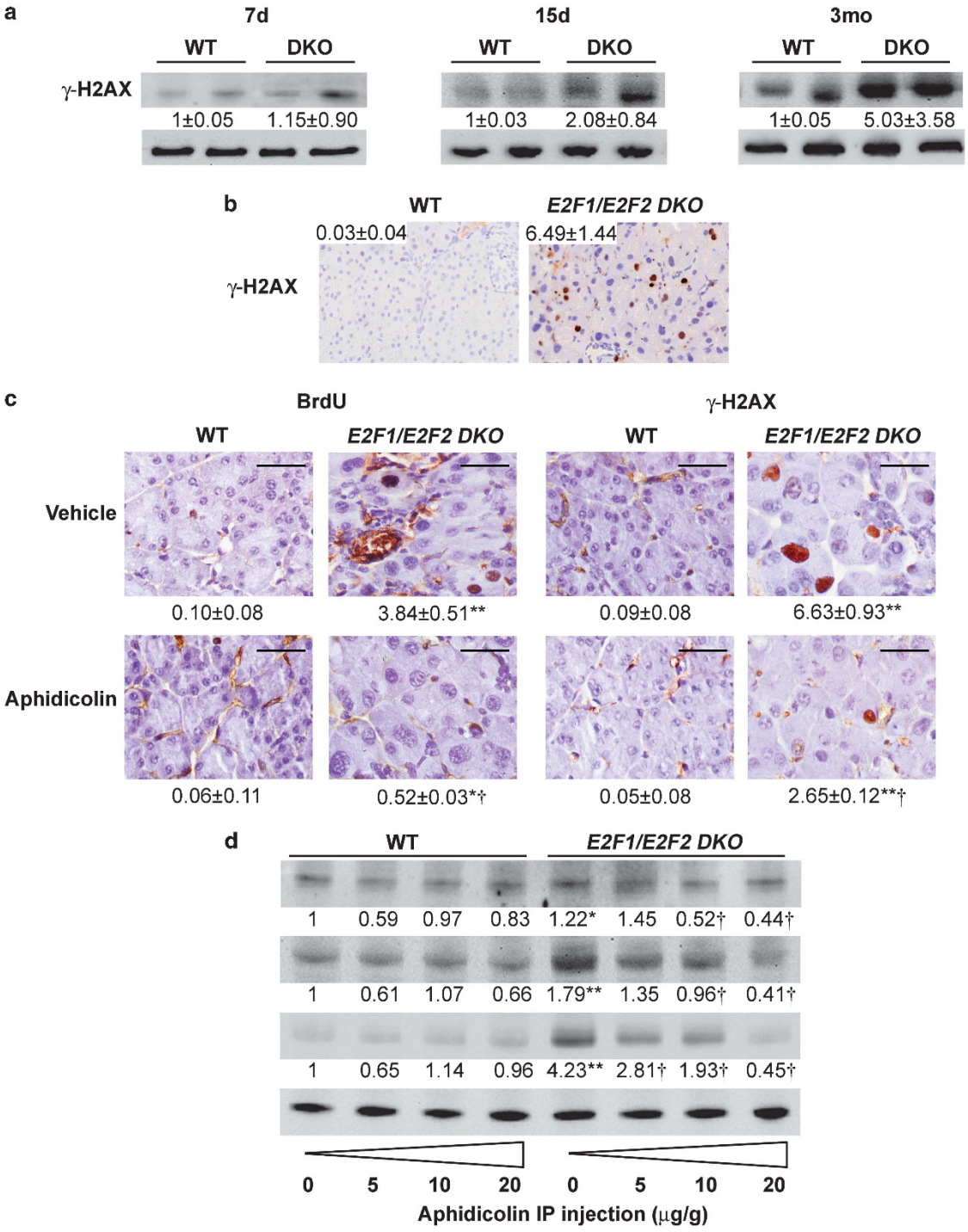

Figure 3 Activation of DDR is triggered by unscheduled DNA replication in cells lacking E2F1 and E2F2. (**a**) Western blot analysis of γ-H2AX in extracts prepared from WT and DKO pancreas collected at different ages. Expression of β-actin was used as a loading control. Numbers below the blots represent normalized densitometric values expressed as fold over WT (mean $\pm$ S.D.). (**b**) Immunohistochemical analysis to identify γ-H2AX-positive nuclei in the pancreas of 2-week-old WT and DKO mice. As shown, DKO mice have an increased number of cells with pan-nuclear γ-H2AX staining (x20). (**c**) *In vivo* BrdU labeling (left panels) and γ-H2AX accumulation (right panels) in pancreases derived from 2-week-old WT and DKO mice, after i.p. injection of vehicle (saline) or aphidicolin. As shown, treatment with aphidicolin (10 μg/g) completely abolishes the incorporation of BrdU and reduces the number of cells with pan-nuclear γ-H2AX staining in DKO cells. The sections shown are representative examples from three mice per treatment (x40). Scale bar indicates 40 μm. The numbers below each figure represent the percentage of BrdU-positive nuclei and γ-H2AX-positive nuclei (mean $\pm$ S.D.) obtained after the analysis of 1000 nuclei in each sample. $^{*}P<0.005$ *versus* untreated WT, $^{**}P<0.0001$ *versus* untreated WT, $^{\dagger}P<0.005$ *versus* untreated DKO. (**d**) Representative western blot analysis of γ-H2AX, p53 and $p21^{CIP1}$ in extracts prepared from pancreas treated with the indicated concentrations of aphidicolin. Expression of β-actin was used as a loading control. Numbers below the blots correspond to the mean densitometric values from three mice per treatment, expressed as fold over WT. $^{*}P<0.05$ *versus* untreated WT, $^{**}P<0.0001$ *versus* untreated WT, $^{\dagger}P<0.005$ *versus* untreated DKO

Immunohistochemical analysis evidenced that over 6% of pancreatic cells were positive for γ-H2AX in 15-day-old DKO mice (Figure 3b). Importantly, γ-H2AX positivity was not observed in organs that undergo scheduled DNA replication, such as the small intestine. Intestinal crypt cells from small intestine exhibited actively replicating DNA in both WT and DKO mice, but no γ-H2AX-positive cells were detected in either genotype (Supplementary Figure1A). Taken together, our results suggest that the unscheduled DNA replication observed in pancreatic cells lacking E2F1/E2F2 may lead to a strong DDR.

To examine the relationship between DNA replication stress and DDR in E2F1/E2F2 mutant pancreas, we treated DKO and WT mice (15–20 days old) with the DNA polymerase inhibitor aphidicolin to inhibit DNA replication *in vivo*.[24] As a control, we showed that *in vivo* administration of aphidicolin was able to reduce DNA replication substantially in the small intestine of both WT and DKO mice (Supplementary Figure 1B). In the pancreas of DKO mice *in vivo* aphidicolin treatment blocked DNA replication, as evidenced by the reduction in bromodeoxyuridine (BrdU) uptake (Figure 3c, left panels). Next, we examined the expression of γ-H2AX by immunohistochemistry. Importantly, aphidicolin reduced the number of cells with γ-H2AX staining in DKO pancreas (Figure 3c, right panels). Furthermore, western analyses showed that inhibition of DNA replication by aphidicolin prevented the accumulation of p53 and $p21^{CIP1}$ in a dose-dependent manner in DKO pancreas (Figure 3d). We conclude that the abnormal DNA replication and the resulting replication stress trigger DDR and subsequent activation of p53 pathway in DKO pancreas.

$p21^{CIP1}$ is dispensable for the aberrant pancreatic phenotype developed by cells lacking E2F1/E2F2. We next analyzed the contribution of the pathways governed by p53 and its transcriptional target $p21^{CIP1}$ to the atrophy of DKO pancreas. We first generated E2F1/E2F2/$p21^{CIP1}$ triple-knockout (TKO) mice and examined these mice in parallel with $E2F1^{-/-}$/$E2F2^{-/-}$, $p21^{-/-}$ and wild-type mice. Loss of $p21^{CIP1}$ did not reverse the histological abnormalities previously described in adult DKO pancreases. In fact, these abnormalities were more severe in E2F1/E2F2/$p21^{CIP1}$ TKO mice (Supplementary Figure 2). Consistently, loss of $p21^{CIP1}$ did not prevent the overexpression of apoptosis markers, the pancreatic atrophy or the hyperglycemia in E2F1/E2F2 DKO mice (Supplementary Figure 3). Other organs that exhibit involution in DKO mice, such as salivary glands, testicles and hematopoietic system, remained atrophic in the TKO animals (data not shown). These findings suggest that the mechanism that dictates cell death induction and triggers organ involution in E2F1/E2F2 DKO mice is $p21^{CIP1}$ independent.

Disruption of p53 in E2F1/E2F2-deficient mice prevents apoptosis and restores a normal pancreatic phenotype. We next generated E2F1/E2F2/p53 TKO mice and analyzed these mice in parallel with $E2F1^{-/-}$/$E2F2^{-/-}$, $p53^{-/-}$ and wild-type mice. Importantly, the expression of p53 target genes (*Bax*, *Puma*, *Apaf-1*, *Pidd* and *Dr5*) was down to normal in E2F1/E2F2/p53 TKO pancreases compared with $E2F1^{-/-}$/$E2F2^{-/-}$ samples (Figure 4a). Consistent with this result, compromised mitochondrial membrane potential was completely rescued in pancreatic cells isolated from TKO animals (Figure 4b), and elimination of p53 from E2F1/E2F2 DKO cells restored cell survival (Figure 4c). By contrast, increased BrdU uptake and accumulation of γ-H2AX persisted in E2F1/E2F2/p53 TKO cells (Supplementary Figure 4). These findings place p53 downstream of DNA replication stress signals and upstream of apoptotic pathways after E2F1/2 loss.

Strikingly, elimination of p53 completely prevented loss of insulin- and glucagon-producing cells and restored the expression of α-amylase in E2F1/E2F2 DKO mice (Figure 5). Histological and morphological abnormalities described in DKO pancreas such as loss of normal architecture, lower number of acini and increased number of ductal structures, were completely absent in E2F1/E2F2/p53 TKO mice (Figure 6a). Furthermore, the acinar cell hypertrophy with marked karyomegaly characteristic of DKO pancreases was completely rescued in TKO animals (Figure 6b). Indeed, mean size of the nuclei in TKO pancreatic acinar cells was clearly reduced compared with the mean size of nuclei in DKO cells (3.17 ± 0.72-fold over WT in DKO mice *versus* 1.55 ± 0.24-fold over WT in TKO mice). Endocrine pancreas, which was atrophic in DKO mice, appeared overtly normal when p53 was eliminated (Figures 6 and 7a). Importantly, glucose levels in serum of TKO mice were similar to the levels found in WTs (Figure 7c), suggesting that insulin secreted by pancreas of E2F1/E2F2/p53 TKO mice is sufficient to maintain normoglycemia.

Histological as well as functional features of other organs that are severely affected in DKO mice, such as testicles and salivary glands, were also overtly normal in TKO mice, including their ability to generate offspring (Supplementary Figure 5 and data not shown). Taken together, these data indicate that p53 is the crucial mediator of the abnormal phenotype displayed by organs in mice lacking E2F1/E2F2.

Disruption of p53 in E2F1/E2F2 mutant mice shortens lifespan owing to the emergence of thymic lymphomas. Unexpectedly, lifespan of TKO mice was found to be significantly shorter than that of WT or $p53^{-/-}$ mice (Figure 8a), even though TKO mice were normoglycemic and showed normal gland structure (Figures 6 and 7). While performing the necropsies we noted that the thymus was severely hypertrophic in E2F1/E2F2/p53 TKO mice. Relative thymus weight in TKO mice was 6-fold higher than that of WT or DKO mice (Figures 8b and c), suggesting that the reduced survival rate of TKO animals stems from a respiratory failure due to thymic tumor growth, as demonstrated for $p53^{-/-}$ mice.[25] Histological sections of TKO thymus confirmed the development of T-cell lymphoblastic leukemia/lymphoma in these mice (Figures 8d and e). Taken together, these findings imply that depletion of E2F1/2 is not only unable to suppress tumor development, but rather increases the oncogenic potential in normal cells.

Discussion

Here we show that E2F1 and E2F2 are crucial players in an essential pathway involved in the maintenance of a post-mitotic state by limiting the capability of the DNA

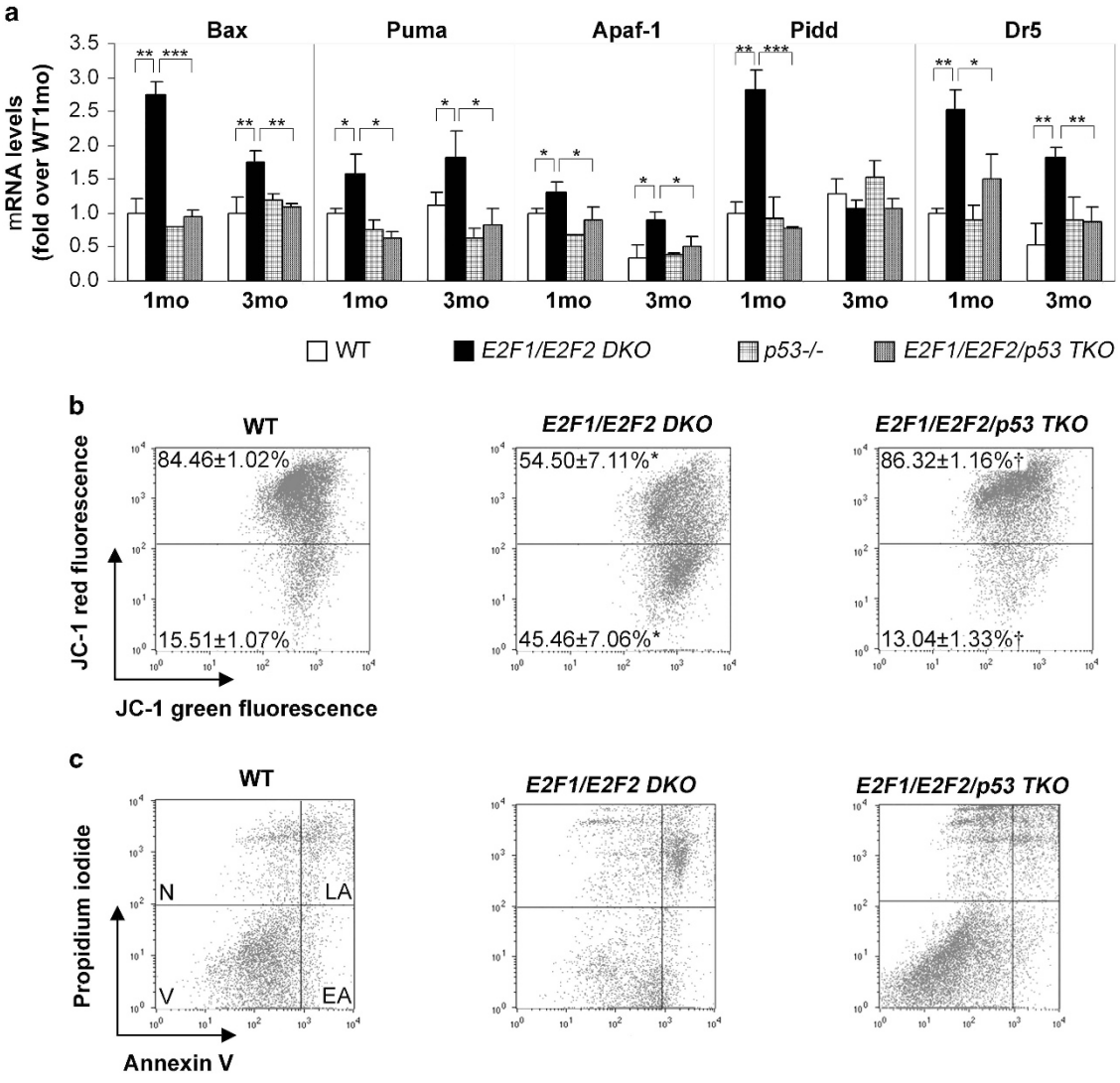

Cell death (%)	WT	*E2F1/E2F2 DKO*	*E2F1/E2F2/p53 TKO*
Early apoptosis (EA)	7.12±1.71	11.20±0.98*	3.46±0.09†
Late apoptosis (LA)	15.32±4.77	26.69±2.12*	13.94±1.88†
Necrosis (N)	12.72±4.21	19.54±0.93	23.20±2.20
Viable (V)	63.89±2.49	42.33±1.59**	59.40±4.29†

Figure 4 Disruption of p53 in E2F1/E2F2 mutant mice prevents apoptosis in pancreas. (**a**) Reverse transcription Q-PCR analysis of indicated genes in WT, E2F1/E2F2 DKO, $p53^{-/-}$ and E2F1/E2F2/p53 TKO pancreas. *Gapdh* was used as a normalization control. Results are expressed as fold over 1-month-old WT (mean ± S.D.) from three mice per age and genotype. $^{*}P<0.05$, $^{**}P<0.01$, $^{***}P<0.0001$. (**b**) FACS analysis on freshly isolated pancreatic cells derived from 15-day-old mice stained with JC-1. Numbers inside each panel represent the percentage of cells (mean ± S.D.) with normal or compromised mitochondrial membrane potential from three independent experiments. $^{*}P<0.05$ *versus* WT, $^{\dagger}P<0.002$ *versus* DKO. (**c**) Apoptotic death in 15-day-old pancreatic cells assessed by Annexin V-FITC and PI staining followed by FACS analysis. Different stages of apoptosis were distinguished as follows: early apoptosis (Annexin V+/PI −); late apoptosis (Annexin V+/PI+); necrosis (Annexin V −/PI+) and viable cells (Annexin V −/PI −). In the table below, results are expressed as % of cells (mean ± S.D.) from three independent experiments. $^{*}P<0.05$ *versus* WT, $^{**}P<0.0001$ *versus* WT, $^{\dagger}P<0.001$ *versus* DKO

replication and cell cycle progression machinery. Failure of this control mechanism results in exacerbated CDK activity and inappropriate DNA replication that induces a DDR pathway and predisposes cells to tumorigenesis. Consequently, an apoptotic program that affects tissue integrity is activated.

In this work, we have analyzed the pathway that leads to apoptosis in pancreas lacking E2F1 and E2F2. It is known that apoptotic cell death in pancreas may be induced as consequence of diabetes, as aberrantly increased glucose levels trigger both extrinsic and intrinsic apoptotic pathways.[26] Conversely, apoptosis may also be the causal factor in

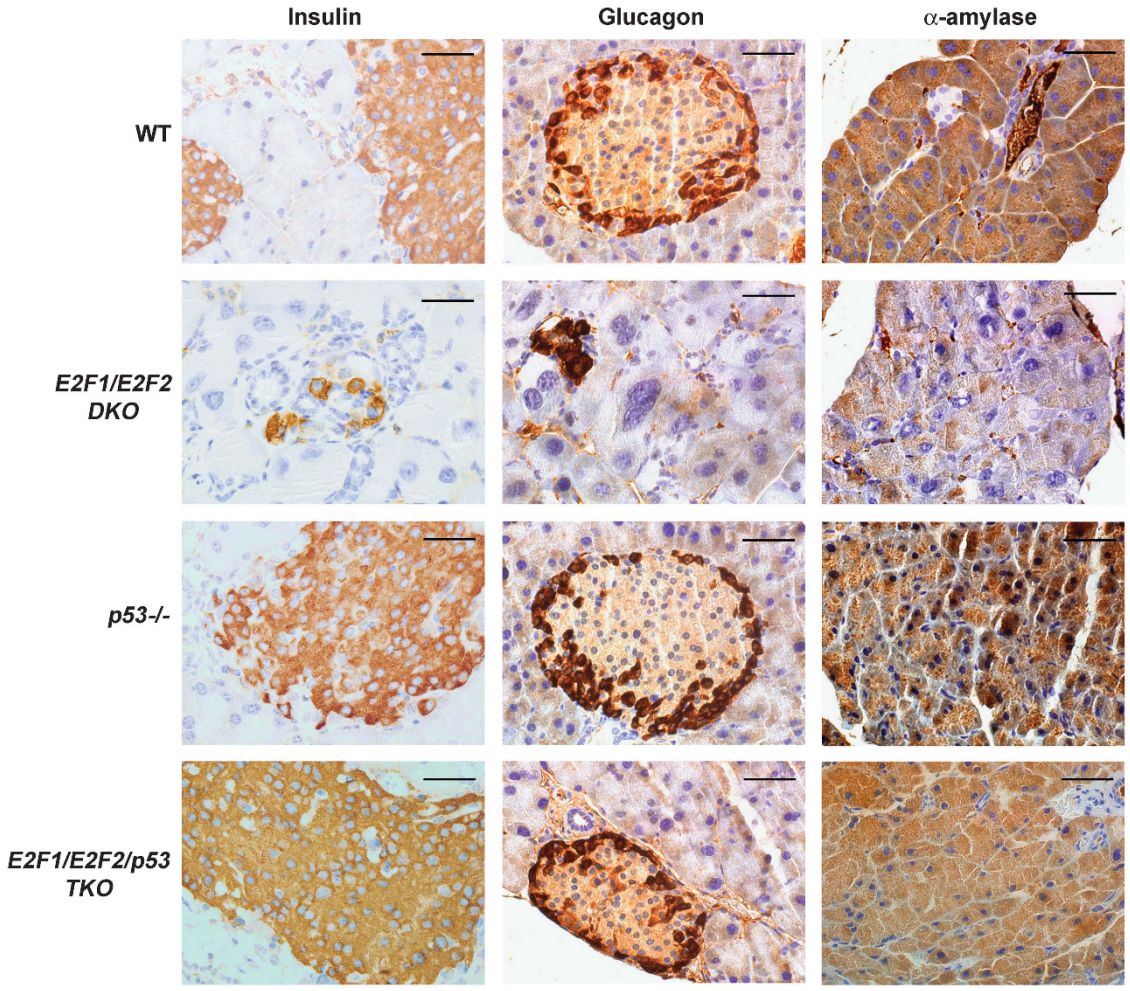

Figure 5 Elimination of p53 in pancreas of E2F1/E2F2 DKO mice restores expression of pancreas-specific protein markers. Representative pancreas sections of 2-month-old WT, E2F1/E2F2 DKO, $p53^{-/-}$ and E2F1/E2F2/p53 TKO mice immunostained with antibodies to insulin, glucagon and α-amylase. A light hematoxylin counterstaining was performed in all sections for contrast (x40). Scale bar indicates 40 μm. Similar results were obtained in more than 10 mice per genotype

diabetes development, as shown in $Perk^{-/-}$ and Pdx-$1^{-/-}$ mouse models of diabetes.[27–30] In E2F1/E2F2-deficient cells, altered expression of proapoptotic mediators and mitochondrial membrane depolarization preceded the onset of diabetes, suggesting that apoptosis is a triggering event for pancreatic degeneration and diabetes in our mouse model. Furthermore, our results demonstrate that apoptosis in mice lacking E2F1/E2F2 is exclusively dependent on p53, since targeted inactivation of p53 hinders apoptosis and restores normal pancreas phenotype. Additionally, the fact that elimination of $p21^{CIP1}$ does not rescue the phenotype of DKO cells suggests that the program elicited by p53 in DKO mice is not primarily aimed to arrest cell cycle, but to activate apoptosis.

Our data strongly suggest that activation of p53 pathway in DKO cells is associated with their aberrant DNA replication. Accumulating experimental evidence indicates that p53 can be activated as part of the DDR pathway triggered by replicative stress.[31] Moreover, abnormal DNA replication leading to p53-dependent apoptosis and inner ear involution occurs after concomitant inactivation of $p19^{ARF}$ and $p21^{CIP1}$ CDKis.[32] In line with these studies, our data showing that *in vivo* inhibition of DNA replication dose dependently prevents activation of the DDR and accumulation of p53 provide support for the notion that replication stress has a major causative role in p53 activation in cells lacking E2F1 and E2F2.

DKO pancreas is overtly normal until the second week of postnatal age,[19] suggesting that E2F1 and E2F2 are dispensable for the timely cellular proliferation occurring up to this age in pancreas. During terminal differentiation, in contrast, they appear to have a major role as repressors of the cell cycle by promoting attenuation of DNA replication. Similar findings have been reported for differentiating monocyte and intestinal epithelial cells.[13,17] However, the cell fates in these cases are different from those observed in pancreatic tissue, as monocyte progenitor cells lacking E2F1/2 result in senescence, and intestinal progenitor cells lacking E2F1-3 lead to p53-independent apoptosis. The mechanism that leads to replication stress in DKO cells is still unknown, and it would be interesting to determine whether it involves illegitimate replication origin firing and fork stalling, as shown for replication stress caused by overexpression of Cdt1[33] or by aberrant CDK activity[34] in some cell types.

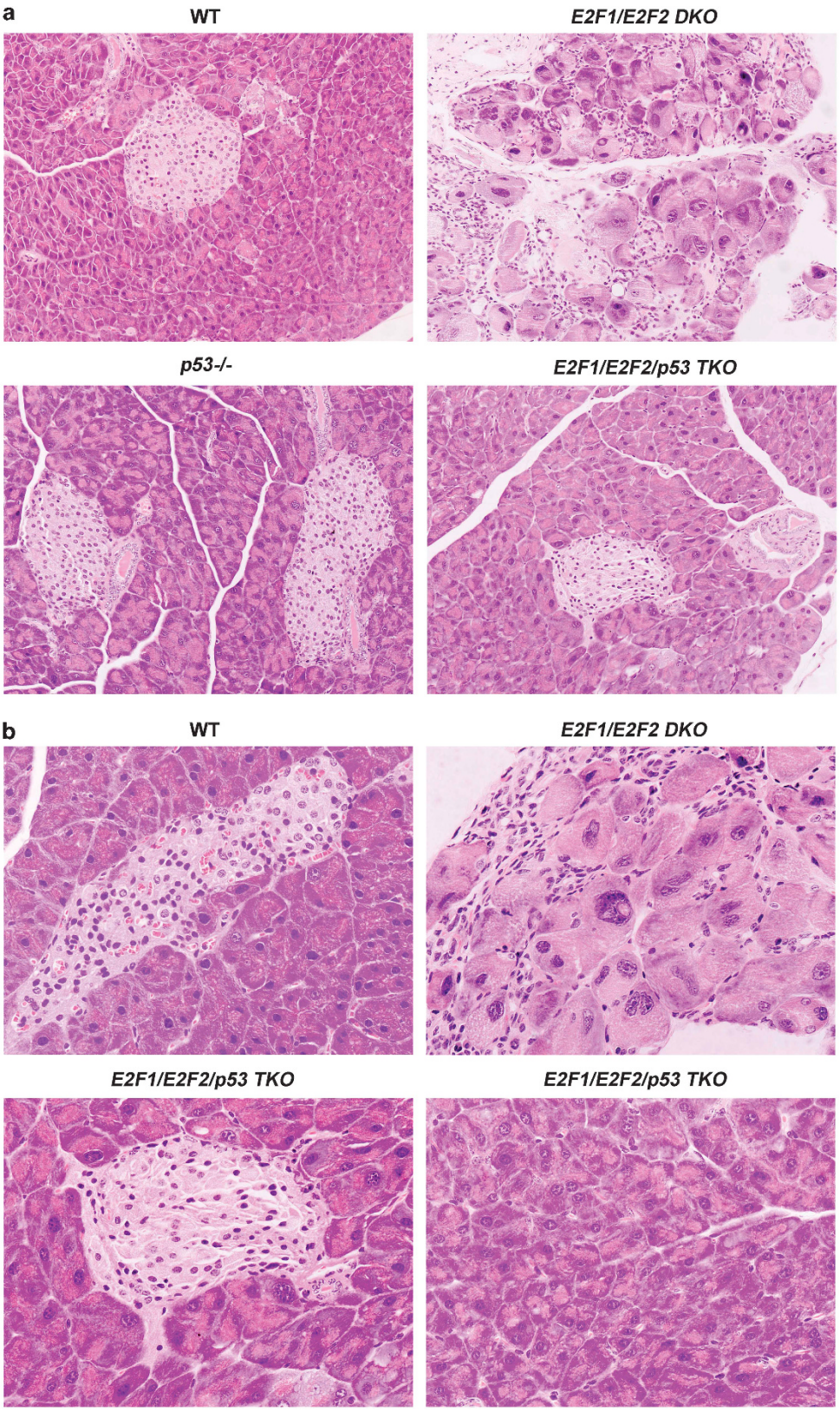

Figure 6 Disruption of p53 in E2F1/E2F2 mutant mice restores normal pancreatic histological appearance. (**a**) Representative sections of pancreas from 2-month-old WT, E2F1/E2F2 DKO, $p53^{-/-}$ and E2F1/E2F2/p53 TKO mice stained with hematoxylin/eosin (x20). (**b**) Representative sections of pancreas from 2-month-old WT, E2F1/E2F2 DKO and E2F1/E2F2/p53 TKO mice stained with hematoxylin/eosin (x40). Note the presence of islets (lower left panel) and acini (lower right panel) in TKO pancreas with a morphology similar to that found in WT animals. The sections shown are representative examples of more than 10 mice per genotype

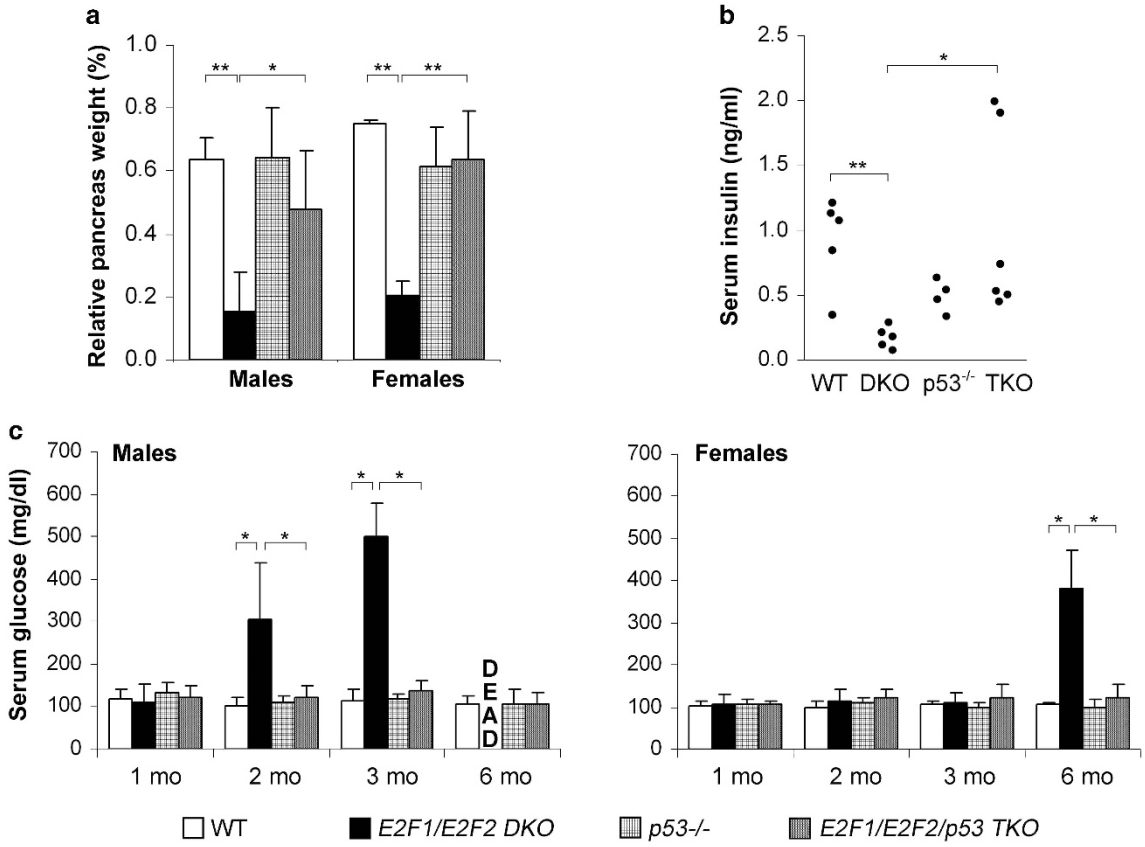

Figure 7 Disruption of p53 in E2F1/E2F2 mutant mice prevents pancreatic atrophy, insulin deficiency and hyperglycemia. (**a**) Pancreas weight expressed as a fraction of total body weight of 3- to 4-month-old animals. Means ± S.D. for 3–5 mice per sex and genotype are shown. $^{*}P<0.05$, $^{**}P<0.0001$. (**b**) Insulin levels in serum of 3-month-old male mice ($n=5$ per genotype, $^{*}P<0.05$, $^{**}P<0.005$). (**c**) Spot blood glucose levels were determined at the indicated times. Results are the means ± S.D. for 5–10 animals per sex, age and genotype. $^{*}P<0.0001$

A controlled CDK activity is key to maintain genome integrity during S phase,[35] and it has been reported that most of the DNA replication stress arises as a result of elevated CDK activity.[36] Interestingly, this phenotype can be alleviated by nucleotide addition.[34,37] In E2F1$^{-/-}$/E2F2$^{-/-}$ cells, overexpression of replication proteins such as Mcm3, Cdc6 and Orc1, together with the increased Cyclin/CDK activity, could be the source of the observed DNA damage. It remains, however, to be determined what the contributing role of CDK activity in unscheduled DNA replication is, and the role of intracellular nucleotide pools in DKO phenotype.

Many of the features exhibited by the E2F1/E2F2 mutant mouse model are similar to those exhibited by aging animals, including general tissue atrophy and degeneration.[38] Interestingly, animal models of progeria have also shown that the absence of p53 relieves some of the growth disadvantages of aging and enhances the lifespan of these animals, unless cancer arises.[39] Individuals with rare genetic diseases that accelerate aging, such as Werner or MDP (Mandibular hypoplasia, Deafness and Progeroid features) syndromes are also known to develop tissue degeneration that affects many organs including the pancreatic gland. Intriguingly, these two syndromes are the result of mutations in genes involved in DNA replication, WRN helicase and DNA polymerase δ catalytic subunit encoding gene *POLD1*, respectively,[40,41] suggesting that DNA replication stress, such as that exhibited by E2F1/2-deficient cells, may drive tissue involution and aging in some pathological conditions.

E2F1 and E2F2 represent controversial players in cell-cycle control, exhibiting dual behavior as tumor suppressors or as oncogenes. Excess of E2F1 may promote proliferation, but may also enhance apoptosis, and there are numerous examples in which deregulation of E2F1 can have both positive and negative effects on tumor growth.[42] Specifically, in pancreatic cancer cell lines, E2F1 is necessary for expression of cancer cell markers, such as Muc4.[43] Conversely, ectopic E2F1 expression in combination with chemotherapeutic drugs results in a strong induction of apoptosis in pancreatic cancer cells.[44] E2F2 has been studied to a lesser extent, but there is evidence of a similar duality of functions accomplished by this factor.[45,46] This dual role of E2Fs seems to depend on the level of E2F activity, but also on the cell context background, greatly influenced by the presence or absence of pRb and/or p53.[6] Our results showing that depletion of E2F1/2 can generate apoptotic signals in cells but promote tumor development upon loss of p53 are consistent with this notion. Inactivation of p53 in E2F1-3-deficient fibroblasts has also been shown to result in transformation of this cell type,[47] implying a general role for the E2F-p53 axis in malignancy. Thus, exacerbating DNA replication rates either by inactivating pRb,[48] or, paradoxically, by depleting E2F1/2 could lead to atrophy in a p53-competent context, but be oncogenic in a p53-deficient context. These

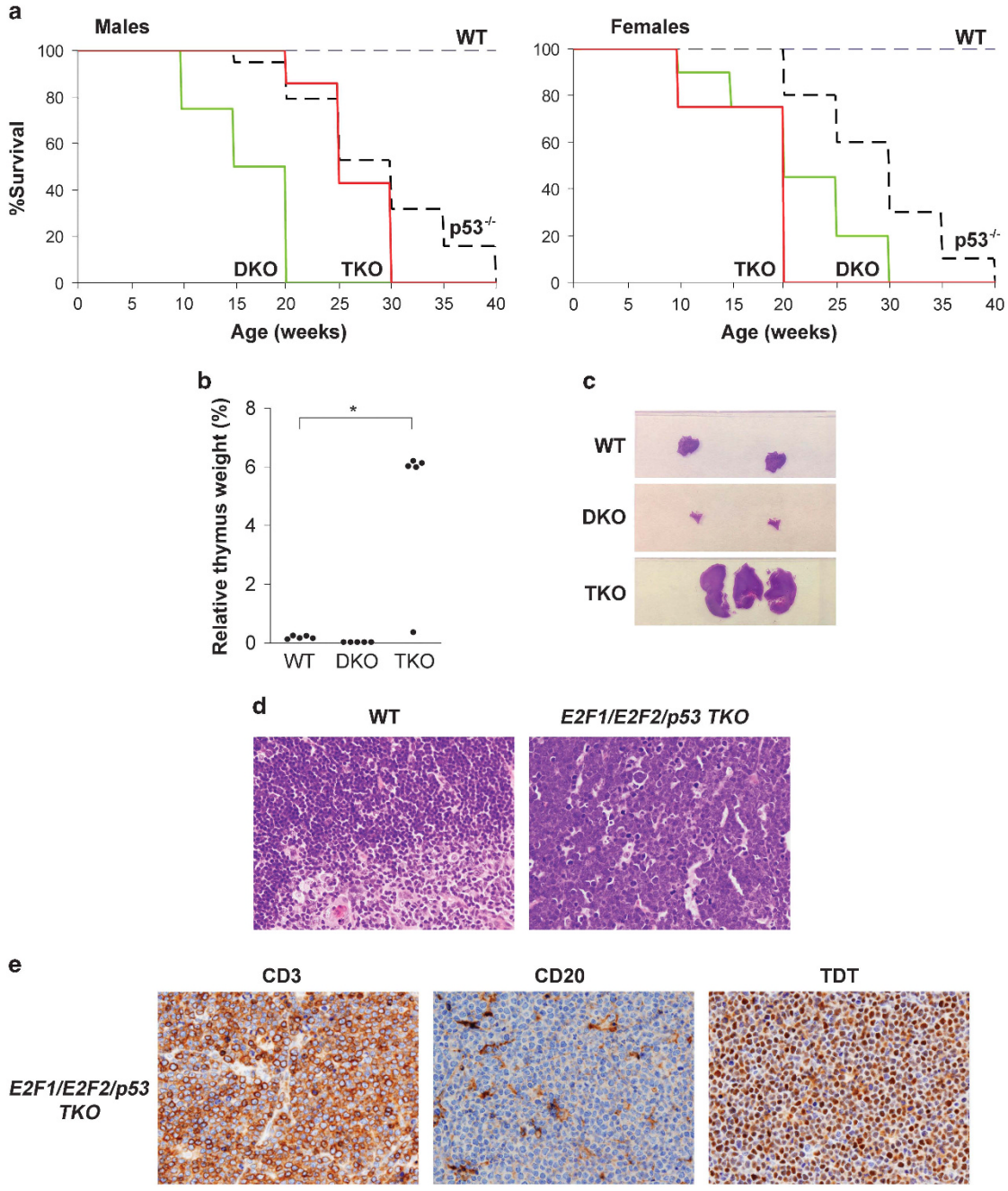

Figure 8 Disruption of p53 in E2F1/E2F2 mutant mice promotes development of thymic lymphomas and compromises survival. (**a**) Life spans of WT, E2F1/E2F2 DKO, $p53^{-/-}$ and E2F1/E2F2/p53 TKO mice ($n=15$/genotype) analyzed using a log-rank non-parametric test and expressed as Kaplan–Meier survival curves (E2F1/E2F2 DKO *versus* WT, $P<0.0001$; E2F1/E2F2/p53 TKO *versus* WT, $P<0.0001$; E2F1/E2F2/p53 TKO *versus* E2F1/E2F2 DKO, $P<0.0001$; E2F1/E2F2/p53 TKO *versus* $p53^{-/-}$, $P<0.0001$). (**b**) Thymus weight expressed as fraction of total body weight in 4- to 6-month-old animals ($n=5$ per genotype, $^{*}P<0.0001$). (**c**) Representative thymus organs obtained from of 6-month-old WT, E2F1/E2F2 DKO and E2F1/E2F2/p53 TKO animals. (**d**) Thymus sections obtained from 6-month-old WT and E2F1/E2F2/p53 TKO animals stained with hematoxylin/eosin (H/E, x40). Note that the typical structure of WT thymus divided into cortex and medulla is completely loss in TKO thymus. (**e**) Immunohistochemical analysis of thymus sections obtained from 6-month-old E2F1/E2F2/p53 TKO animals to detect CD3, CD20 and TDT (x40). Note that E2F1/E2F2/p53 TKO mice exhibit positive staining for CD3 and TDT and negative staining for CD20, implying that TKO mice develop T-cell lymphoblastic leukemia/lymphoma

observations suggest that cells have more than one failsafe mechanism whereby deregulation of one arm of tumor suppression is not sufficient to initiate tumorigenesis, and instead leads to tissue atrophy.

Our findings have implications in the cancer field, given the increasing interest in developing E2F inhibitors for the treatment of cancer. Several studies have shown the usefulness of this approach for inhibition of tumor cell growth.[49,50] Our results indicate that depleting E2F activity in a context in which the pRb and the p53 pathways are functional, which is the situation of most non-cancerous cells in an organism, renders cells susceptible to become

cancerous owing to an increased genomic instability. Thus, both transformed and non-transformed cells should be examined when developing therapeutic approaches targeting E2F for cancer treatment. E2F1/2-deficient mice could constitute a useful model in which to study the mechanisms regulating the control of malignant transformation as well as tissue degeneration in both normal and cancer cells.

Materials and Methods

Mouse strains. Colonies of E2F1$^{-/-}$, E2F2$^{-/-}$ and DKO E2F1$^{-/-}$/E2F2$^{-/-}$ mice have been described.[19,51,52] p53$^{-/-}$ and p21$^{CIP1-/-}$ mice have also been described.[25,53] DKO E2F1$^{-/-}$/E2F2$^{-/-}$ mice were bred to p53$^{-/-}$ or p21$^{CIP1-/-}$ mice to generate TKO E2F1$^{-/-}$/E2F2$^{-/-}$/p53$^{-/-}$ or E2F1$^{-/-}$/E2F2$^{-/-}$/p21$^{CIP1-/-}$ animals. All procedures were approved by the University of the Basque Country Animal Care and Use Committee.

Metabolic studies. Blood glucose levels were determined from blood taken from mouse tails, using an automatic glucose monitor. Blood for insulin levels was collected from the submandibular vein. Insulin levels were measured in serum by ELISA (ALPCO Diagnostics, Windham, NH, USA), according to the manufacturer's instructions.

Amount of ROS in pancreas was determined in liquid nitrogen-frozen pancreases, using OxiSelect *In Vitro* ROS/RNS Assay Kit (Cell Biolabs, San Diego, CA, USA) according to the protocol of the manufacturer.

Histology, immunohistochemistry and *in vivo* S-phase labeling. Freshly collected tissues were fixed with 10% formalin in PBS and embedded in paraffin for staining with hematoxilin and eosin.

Immunohistochemical assays were performed on tissues fixed with 4% paraformaldehyde in PBS using the indirect immunoperoxidase detection protocol EnvisionFLEX (DAKO A/S, Glostrup, Denmark) in the automatic system DAKO autostainer link 48 (DAKO). The antibodies used were rabbit mAbs to glucagon (1 : 300; DAKO), Terminal Deoxynucleotidyl Transferase (TDT) (1 : 50; DAKO), γ-H2AX (1 : 2000; Millipore, Billerica, MA, USA), and mouse mAbs to insulin (1 : 3,000), α-amylase (2 μg/ml) (Sigma-Aldrich, St. Louis, MO, USA), CD3 (1 : 50; DAKO) and CD20 (1 : 400; DAKO). Control immunostainings using the secondary antibody in the absence of the primary antibody were routinely performed.

For S-phase labeling, mice were injected intraperitoneally (i.p.) with BrdU (Sigma) (50 μg/g of body weight). Mouse organs were harvested 8 h later, and fixed in 10% formalin. Tissue sections were processed for inmunohistochemistry using the rabbit monoclonal mAb to BrdU (1 : 100; DAKO). Images were captured using Olympus Cell B software (Digital Image Systems, Athens, Greece).

WT and DKO mice were injected i.p. with 5–120 μg/g aphidicolin (Sigma). Controls received an equivalent volume of normal saline i.p. After 30 min, mice were injected i. p. with BrdU. Mouse organs were harvested 4 h after the injection with aphidicolin. Freshly collected tissues were divided into two pieces and one set was fixed with 10% formalin in PBS and embedded in paraffin, whereas the other set was placed immediately in liquid nitrogen to perform protein extraction.

Immunofluorescence of pH3 was performed on frozen tissue sections. Slides were microwaved at boiling for 30 min in 10 mM citric acid buffer, pH 6.0 and allowed to cool (30 min) before 5 min washes in 50 mM TBS, 0.1% Tween-20 (pH 7.4). Tissue sections were immunostained using primary antibody against pH3 (Ser15; Upstate, Millipore) and Alexa Fluor 594 (Molecular Probes, Carlsbad, CA, USA) secondary antibody. DNA was counterstained with Hoechst 33288 dye and analysis was performed using an Olympus Fluoview FV500 microscope (Olympus America, Center Valley, PA, USA) and Olympus Fluoview 1.7b software (Olympus America).

Image J Software from NIH (National Institutes of Health, Bethesda, MD, USA) was used to determine the percentage of BrdU+, γ-H2AX+ or pH3+ nuclei in images of three randomly selected fields (×20 magnification) from 2 to 4 pancreases per genotype.

Pancreatic cell isolation. Individual pancreatic cells were prepared essentially as previously described.[54] Briefly, 2.5 ml of 0.3 mg/ml collagenase solution (*Clostridium histolyticum*; Roche, Nutley, NJ, USA) in KHB, pH 7.4 (118 mM NaC1, 25 mM $NaHCO_3$, 4.7 mM KC1, 1.1 mM $MgCl_2$,, 2.5 mM $CaCl_2$, 1.2 mM $NaHPO_4$, and 14 mM glucose) was injected into the pancreas with a 27 gauge needle, and the gland was incubated at 37 °C in a 15-ml polythene flask containing additional 2.5 ml of collagenase solution. After 20 min, the solution was replaced with KHB lacking Mg^{2+} and Ca^{2+} and containing 2 mM EDTA and incubated for 3 min. The solution was then replaced with fresh calcium-free KHB and the tissue was incubated for a further 3 min. This was followed by a final incubation in collagenase in calcium-containing KHB for 20–30 min, until mostly single cells were present. The tissue was then further dispersed and filtered through a 100-μm nylon mesh (Spectrum Laboratories, Rancho Dominguez, CA, USA).

Analysis of mitochondrial membrane potential, mitochondrial mass and apoptosis. Mitochondrial membrane potential was measured using the lipophilic cationic probe JC-1 as described.[55] JC-1 dye was purchased from Molecular Probes (Leiden, The Netherlands) and stored in DMSO (Sigma). Cells were adjusted to a density of 1×10^6/ml and stained with 3 μM JC-1 for 15 min at 37 °C. The mitochondrial uncoupler carbonyl cyanide m-chloro phenyl hydrazone (CCCP, Molecular Probes) was used at 50 μM for 5 min previous to incubation with JC-1 dye as a control to measure compromised mitochondrial membrane potential. Cells were then washed twice with pre-warmed KHB buffer and resuspended in KHB. Fluorescence was detected and analyzed using a FACSCalibur flow cytometer (Becton & Dickinson, San Jose, CA, USA).

To detect mitochondrial mass, NAO was used as described elsewhere.[56] Briefly, cells were incubated at the concentration of 0.5×10^6/ml with 5 μM NAO for 10 min at 37 °C, washed twice in cold KHB and analyzed using a FACSCalibur flow cytometer.

Apoptosis was measured in freshly isolated acinar cells with the Annexin V-FITC Apoptosis Detection KIT II (BD Pharmingen, Becton & Dickinson) and analyzed by flow cytometry.

Quantitative RT-PCR analysis. Total RNA was isolated from pancreatic tissue with Trizol reagent (Invitrogen, Life Technologies, Carlsbad, CA, USA), according to the manufacturer's instructions, purified using the RNeasy kit (Qiagen, Redwood City, CA, USA) and electrophoresed on a denaturing agarose gel to examine for RNA integrity. cDNA was synthesized from 2.5 μg of RNA using High Capacity cDNA Reverse Transcription Kit (Applied Biosystems, Carlsbad, CA, USA) and all samples were diluted to the same final cDNA concentration. Real-time PCR was performed on several cDNA dilutions plus 1× SYBR green PCR Master Mix (Applied Biosystems) and 300–900 nM of primers for the analyzed genes (sequences in Supplementary Table). Reactions were carried out using an ABI Prism 7000 SDS (Applied Biosystems) for 40 cycles (95 °C for 15 s and 60 °C for 1 min) after an initial 10-min incubation at 95 °C. Relative amounts of cDNA were normalized to the internal control *Gapdh*, whose levels were invariant in all the analyzed genotypes.

Protein extraction and western blot analysis. Total pancreatic homogenates were prepared as described[57] in liquid nitrogen in a mortar cooled in a bath of methanol with dry ice. The powder was transferred to a tube and proteins were solubilized in lysis buffer (1% SDS, 25 mM Tris pH 7.5, 1 mM EGTA pH 8, 1 mM EDTA pH 8, 2 mM pefabloc, 10 μg/ml leupeptin, 10 μg/ml pepstatin, 10 μg/ml benzamidine, 10 μg/ml aprotinin and 10 mM sodium orthovanadate). After vortexing, extracts were boiled for 15 min, centrifuged at 13 000 r.p.m. for 5 min at 4 °C, and the pellet was discarded. Western blots were performed with 20 μg of total protein extract per lane, using antibodies against Apex1 (Novus Biologicals, Littleton, CO, USA), acetylated p53 (Lys 382), phosphorylated pRb (Ser 807/811 and Ser 780), Cyclin B1, phosphorylated Cdk1 (Tyr 15) (Cell Signalling, Danvers, MA, USA), phospho-histone H2AX (Ser 139, Millipore), p53, p19, p21, pRb, Cdk1, Wee1, Cdc25c and β-actin (Santa Cruz Biotechnologies, Santa Cruz, CA, USA). Immunocomplexes were visualized with horseradish peroxidase-conjugated anti-mouse or anti-rabbit IgG antibodies (Amersham), followed by chemiluminiscence detection (ECL, Amersham, GE Healthcare Bio-Sciences, Pittsburgh, PA, USA) with a ChemiDoc camera (Bio-Rad Laboratories, Hercules, CA, USA). Semi-quantitative analysis was performed using Quantity One (Bio-Rad Laboratories).

Statistical analysis. Data are given as mean $\pm$ S.D. Statistical analysis was performed using ANOVA and Fisher's test. Significance was defined by $P < 0.05$.

Acknowledgements. We thank members of the Zubiaga laboratory for helpful discussions, Asier Garcia Senosain for technical support in the analysis of oxidative stress, Oskar Fernandez-Capetillo for the advising with γ-H2AX detection by immunohistochemistry, Jon Fernandez-Rueda for helping with E2F1/E2F2/p21$^{-/-}$ mice, Naiara Zorrilla, Iván Gómez and Santiago Montes for technical support and Jose Antonio Rodriguez for critical reading of the manuscript. OZ is recipient of

Basque Government fellowship for graduated studies. This work was supported by grants from the Spanish Ministry (SAF2012-33551), the Basque Government (IE12-331 and IT634-13), and the University of the Basque Country UPV/EHU (UFI11/20) to AMZ, and from the Spanish Ministry (SAF2012-34059, co-funded by the European Regional Development Fund, and IPT2011-1527-010000, associated to Fibrostatin SL) to JM.

1. Weinberg RA. The retinoblastoma protein and cell cycle control. *Cell* 1995; **81**: 323–330.
2. Sherr CJ. Ink4-arf locus in cancer and aging. *Wiley Interdiscip Rev Dev Biol* 2012; **1**: 731–741.
3. Tyner SD, Venkatachalam S, Choi J, Jones S, Ghebranious N, Igelmann H *et al.* P53 mutant mice that display early ageing-associated phenotypes. *Nature* 2002; **415**: 45–53.
4. Trimarchi JM, Lees JA. Sibling rivalry in the E2F family. *Nat Rev Mol Cell Biol* 2002; **3**: 11–20.
5. Hanahan D, Weinberg RA. The hallmarks of cancer. *Cell* 2000; **100**: 57–70.
6. Tsantoulis PK, Gorgoulis VG. Involvement of E2F transcription factor family in cancer. *Eur J Cancer* 2005; **41**: 2403–2414.
7. DeGregori J, Kowalik T, Nevins JR. Cellular targets for activation by the E2F1 transcription factor include DNA synthesis- and G1/S-regulatory genes. *Mol Cell Biol* 1995; **15**: 4215–4224.
8. Attwooll C, Lazzerini Denchi E, Helin K. The E2F family: specific functions and overlapping interests. *EMBO J* 2004; **23**: 4709–4716.
9. van den Heuvel S, Dyson NJ. Conserved functions of the pRB and E2F families. *Nat Rev Mol Cell Biol* 2008; **9**: 713–724.
10. Müller H, Bracken AP, Vernell R, Moroni MC, Christians F, Grassilli E *et al.* E2Fs regulate the expression of genes involved in differentiation, development, proliferation, and apoptosis. *Genes Dev* 2001; **15**: 267–285.
11. Infante A, Laresgoiti U, Fernández-Rueda J, Fullaondo A, Galán J, Díaz-Uriarte R *et al.* E2F2 represses cell cycle regulators to maintain quiescence. *Cell Cycle* 2008; **7**: 3915–3927.
12. Morris EJ, Ji JY, Yang F, Di Stefano L, Herr A, Moon NS *et al.* E2F1 represses beta-catenin transcription and is antagonized by both pRB and CDK8. *Nature* 2008; **455**: 552–556.
13. Chong JL, Wenzel PL, Saenz-Robles MT, Nair V, Ferrey A, Hagan JP *et al.* E2f1-3 switch from activators in progenitor cells to repressors in differentiating cells. *Nature* 2009; **462**: 930–934.
14. Bueno MJ, Gomez de Cedron M, Laresgoiti U, Fernandez-Piqueras J, Zubiaga AM, Malumbres M *et al.* Multiple E2F-induced microRNAs prevent replicative stress in response to mitogenic signaling. *Mol Cell Biol* 2010; **30**: 2983–2995.
15. Lee BK, Bhinge AA, Iyer VR. Wide-ranging functions of E2F4 in transcriptional activation and repression revealed by genome-wide analysis. *Nucleic Acids Res* 2011; **39**: 3558–3573.
16. Helin K. Regulation of cell proliferation by the E2F transcription factors. *Curr Opin Genet Dev* 1998; **8**: 28–35.
17. Iglesias-Ara A, Zenarruzabeitia O, Fernandez-Rueda J, Sanchez-Tillo E, Field SJ, Celada A *et al.* Accelerated DNA replication in E2F1- and E2F2-deficient macrophages leads to induction of the DNA damage response and p21(CIP1)-dependent senescence. *Oncogene* 2010; **29**: 5579–5590.
18. Li FX, Zhu JW, Tessem JS, Beilke J, Varella-Garcia M, Jensen J *et al.* The development of diabetes in E2f1/E2f2 mutant mice reveals important roles for bone marrow-derived cells in preventing islet cell loss. *Proc Natl Acad Sci USA* 2003; **100**: 12935–12940.
19. Iglesias A, Murga M, Laresgoiti U, Skoudy A, Bernales I, Fullaondo A *et al.* Diabetes and exocrine pancreatic insufficiency in E2F1/E2F2 double-mutant mice. *J Clin Invest* 2004; **113**: 1398–1407.
20. Heller RS, Stoffers DA, Bock T, Svenstrup K, Jensen J, Horn T *et al.* Improved glucose tolerance and acinar dysmorphogenesis by targeted expression of transcription factor PDX-1 to the exocrine pancreas. *Diabetes* 2001; **50**: 1553–1561.
21. Aslanian A, Iaquinta PJ, Verona R, Lees JA. Repression of the arf tumor suppressor by E2F3 is required for normal cell cycle kinetics. *Genes Dev* 2004; **18**: 1413–1422.
22. Chen D, Pacal M, Wenzel P, Knoepfler PS, Leone G, Bremner R *et al.* Division and apoptosis of E2f-deficient retinal progenitors. *Nature* 2009; **462**: 925–929.
23. Tell G, Damante G, Caldwell D, Kelley MR. The intracellular localization of APE1/Ref-1: more than a passive phenomenon? *Antioxid Redox Signal* 2005; **7**: 367–384.
24. O'Dwyer PJ, Moyer JD, Suffness M, Harrison Jr SD, Cysyk R, Hamilton TC *et al.* Antitumor activity and biochemical effects of aphidicolin glycinate (NSC 303812) alone and in combination with cisplatin *in vivo*. *Cancer Res* 1994; **54**: 724–729.
25. Donehower LA, Harvey M, Slagle BL, McArthur MJ, Montgomery Jr CA, Butel JS *et al.* Mice deficient for p53 are developmentally normal but susceptible to spontaneous tumours. *Nature* 1992; **356**: 215–221.
26. Maedler K, Donath MY. Beta-cells in type 2 diabetes: a loss of function and mass. *Horm Res* 2004; **62**: 67–73.
27. Harding HP, Zeng H, Zhang Y, Jungries R, Chung P, Plesken H *et al.* Diabetes mellitus and exocrine pancreatic dysfunction in perk −/− mice reveals a role for translational control in secretory cell survival. *Mol Cell* 2001; **7**: 1153–1163.
28. Johnson JD, Ahmed NT, Luciani DS, Han Z, Tran H, Fujita J *et al.* Increased islet apoptosis in Pdx1+/− mice. *J Clin Invest* 2003; **111**: 1147–1160.
29. Oyadomari S, Koizumi A, Takeda K, Gotoh T, Akira S, Araki E *et al.* Targeted disruption of the chop gene delays endoplasmic reticulum stress-mediated diabetes. *J Clin Invest* 2002; **109**: 525–532.
30. Donath MY, Halban PA. Decreased beta-cell mass in diabetes: significance, mechanisms and therapeutic implications. *Diabetologia* 2004; **47**: 581–589.
31. d'Adda di Fagagna F. Living on a break: cellular senescence as a DNA-damage response. *Nat Rev Cancer* 2008; **8**: 512–522.
32. Laine H, Doetzlhofer A, Mantela J, Ylikoski J, Laiho M, Roussel MF *et al.* p19(Ink4d) and p21 (Cip1) collaborate to maintain the postmitotic state of auditory hair cells, their codeletion leading to DNA damage and p53-mediated apoptosis. *J Neurosci* 2007; **27**: 1434–1444.
33. Davidson IF, Li A, Blow JJ. Deregulated replication licensing causes DNA fragmentation consistent with head-to-tail fork collision. *Mol Cell* 2006; **24**: 433–443.
34. Beck H, Nahse-Kumpf V, Larsen MS, O'Hanlon KA, Patzke S, Holmberg C *et al.* Cyclin-dependent kinase suppression by WEE1 kinase protects the genome through control of replication initiation and nucleotide consumption. *Mol Cell Biol* 2012; **32**: 4226–4236.
35. Beck H, Nahse V, Larsen MS, Groth P, Clancy T, Lees M *et al.* Regulators of cyclin-dependent kinases are crucial for maintaining genome integrity in S phase. *J Cell Biol* 2010; **188**: 629–638.
36. Sorensen CS, Syljuasen RG. Safeguarding genome integrity: The checkpoint kinases ATR, CHK1 and WEE1 restrain CDK activity during normal DNA replication. *Nucleic Acids Res* 2012; **40**: 477–486.
37. Bester AC, Roniger M, Oren YS, Im MM, Sarni D, Chaoat M *et al.* Nucleotide deficiency promotes genomic instability in early stages of cancer development. *Cell* 2011; **145**: 435–446.
38. Gessert CE, Elliott BA, Haller IV. Dying of old age: An examination of death certificates of minnesota centenarians. *J Am Geriatr Soc* 2002; **50**: 1561–1565.
39. Rodier F, Campisi J, Bhaumik D. Two faces of p53: Aging and tumor suppression. *Nucleic Acids Res* 2007; **35**: 7475–7484.
40. Chen L, Oshima J. Werner syndrome. *J Biomed Biotechnol* 2002; **2**: 46–54.
41. Weedon MN, Ellard S, Prindle MJ, Caswell R, Lango Allen H, Oram R *et al.* An in-frame deletion at the polymerase active site of POLD1 causes a multisystem disorder with lipodystrophy. *Nat Genet* 2013; **45**: 947–950.
42. Johnson DG, Degregori J. Putting the Oncogenic and Tumor Suppressive Activities of E2F into Context. *Curr Mol Med* 2006; **6**: 731–738.
43. Kunigal S, Ponnusamy MP, Momi N, Batra SK, Chellappan SP. Nicotine, IFN-γ and retinoic acid mediated induction of MUC4 in pancreatic cancer requires E2F1 and STAT-1 transcription factors and utilize different signaling cascades. *Mol Cancer* 2012; **11**: 24.
44. Rödicker F, Stiewe T, Zimmermann S, Pützer BM. Therapeutic efficacy of E2F1 in pancreatic cancer correlates with TP73 induction. *Cancer Res* 2001; **61**: 7052–7055.
45. Scheijen B, Bronk M, van der Meer T, De Jong D, Bernards R. High incidence of thymic epithelial tumors in E2F2 transgenic mice. *J Biol Chem* 2004; **279**: 10476–10483.
46. Opavsky R, Tsai SY, Guimond M, Arora A, Opavska J, Becknell B *et al.* Specific tumor suppressor function for E2F2 in Myc-induced T cell lymphomagenesis. *Proc Natl Acad Sci USA* 2007; **104**: 15400–15405.
47. Sharma N, Timmers C, Trikha P, Saavedra HI, Obery A, Leone G *et al.* Control of the p53-p21CIP1 Axis by E2f1, E2f2, and E2f3 is essential for G1/S progression and cellular transformation. *J Biol Chem* 2006; **281**: 36124–36131.
48. Bosco EE, Mayhew CN, Hennigan RF, Sage J, Jacks T, Knudsen ES *et al.* RB signaling prevents replication-dependent DNA double-strand breaks following genotoxic insult. *Nucleic Acids Res* 2004; **32**: 25–34.
49. Ma Y, Kurtyka CA, Boyapalle S, Sung SS, Lawrence H, Guida W *et al.* A small-molecule E2F inhibitor blocks growth in a melanoma culture model. *Cancer Res* 2008; **68**: 6292–6299.
50. Xie X, Bansal N, Shaik T, Kerrigan JE, Minko T, Garbuzenko O *et al.* A novel peptide that inhibits E2F transcription and regresses prostate tumor xenografts. *Oncotarget* 2014; **5**: 901–907.
51. Field SJ, Tsai FY, Kuo F, Zubiaga AM, Kaelin Jr WG, Livingston DM *et al.* E2F-1 functions in mice to promote apoptosis and suppress proliferation. *Cell* 1996; **85**: 549–561.
52. Murga M, Fernandez-Capetillo O, Field SJ, Moreno B, Borlado LR, Fujiwara Y *et al.* Mutation of E2F2 in mice causes enhanced T lymphocyte proliferation, leading to the development of autoimmunity. *Immunity* 2001; **15**: 959–970.
53. Balomenos D, Martín-Caballero J, García MI, Prieto I, Flores JM, Serrano M *et al.* The cell cycle inhibitor p21 controls T-cell proliferation and sex-linked lupus development. *Nat Med* 2000; **6**: 171–176.
54. Amsterdam A, Solomon TE, Jamieson JD. Sequential dissociation of the exocrine pancreas into lobules, acini, and individual cells. *Methods Cell Biol* 1978; **20**: 361–378.
55. Cossarizza A, Baccarani-Contri M, Kalashnikova G, Franceschi C. A new method for the cytofluorimetric analysis of mitochondrial membrane potential using the J-aggregate forming lipophilic cation 5,5',6,6'-tetrachloro-1,1',3,3'-tetraethylbenzimidazolcarbocyanine iodide (JC-1). *Biochem Biophys Res Commun* 1993; **197**: 40–45.
56. Maftah A, Petit JM, Ratinaud MH, Julien R. 10-N nonyl-acridine orange: A fluorescent probe which stains mitochondria independently of their energetic state. *Biochem Biophys Res Commun* 1989; **164**: 185–190.
57. Molero X, Adell T, Skoudy A, Padilla MA, Gomez JA, Chalaux E *et al.* Pancreas transcription factor 1alpha expression is regulated in pancreatitis. *Eur J Clin Invest* 2007; **37**: 791–801.

Supplementary Information accompanies this paper on Cell Death and Differentiation website (http://www.nature.com/cdd)